Kerbala Journal of Pharmaceutical Sciences

ISSN: 2221-7207(Print) / **ISSN**: 3006-7189 (Online)

The Effects of Extreme Electrospinning and Environmental Parameters on the Resulted Zein Nanofibers Formulated by the Electrospinning Technique

Mokhtar A. S. Al-Janabi[1,2], Sarmad S. N. Al-Edresi[1*]

[1] Department of Pharmaceutics and Industrial Pharmacy, Faculty of Pharmacy, University of Kufa, Najaf, Iraq. 52001

[2] Najaf Health Directorate, Al Imam Al Sajjad General Hospital, Najaf, Iraq.

***Corresponding Author:**
Sarmad S. N. Al-Edresi: s.aledresi@uokufa.edu.iq

Received: 02/09/2023

Accepted: 22/12/2023

Published:30/06/2024

Keywords: Zein; Electrospinning; Humidity; Nanofiber; Morphology; Field Emission Scanning Electron Microscope

DOI:10.62472/kjps.v15.i24.11-20

Abstract

Objective: The study declares and shows the effect of electrospinning parameters, including the temperature, humidity, applied voltage, syringe gage, the distance between the needle tip and collector, and flow rate on the morphology of the resulted nanofiber using the electrospinning technique in the preparation of Zein polymer nanofibers.

Methods: The Zein nanofiber was formulated as nanofibers using an electrospinning apparatus. The nanofibers were prepared in different conditions, adjusting the parameters in each single run-in various temperatures and humidity. At the same time, the concentration of the zein polymer remained constant in all of the runs. Then, the nanofibers obtained after drying and collecting them from the aluminum foil were transferred to a tightly sealed container. The nanofiber was characterized using Attenuated Total Reflectance Infrared Spectroscopy (FTIR) to detect the presence of Zein polymer in the matrix. Then, the surface morphology of nanofibers was analyzed using the Scanning Electron Microscopy (SEM) technique. To declare the morphologic changes in the resulting nanofibers.

Results: The results indicate that some specific parameters and conditions can lead to perfectly shaped nanofibers, and applying different conditions and parameters can lead to abnormal morphological topography and electro-spraying instead of electrospun nanofibers.

Conclusions: The SEM images provided visual evidence of the change in morphology that resulted in each different run-in with different conditions and parameters.

Aim of the Study: This study aimed to identify the effect of different electrospinning and environmental parameters on the resulting zein polymer nanofibers.

تأثيرات الغزل الكهربائي الشديد والمعلمات البيئية على ألياف الزين النانوية الناتجة التي تم صياغتها بواسطة تقنية الغزل الكهربائي

مختار الجنابي، سرمد الإدريسي

الملخص

تهدف الدراسة إلى توضيح تأثير معلمات الغزل الكهربائي، بما في ذلك درجة الحرارة والرطوبة والجهد المطبق وعيار الحقنة والمسافة بين رأس الإبرة والمجمع ومعدل التدفق على شكل الألياف النانوية الناتجة باستخدام تقنية الغزل الكهربائي في تحضير ألياف النانو بوليمر الزين.

الطريقة:

تمت صياغة ألياف النانو الزين باستخدام جهاز الغزل الكهربائي. تم تحضير الألياف النانوية في ظروف مختلفة، مع ضبط المعلمات في كل تجربة على درجات حرارة ورطوبة متنوعة. في الوقت نفسه، ظل تركيز بوليمر الزين ثابتًا في جميع التجارب. بعد ذلك، تم نقل الألياف النانوية التي تم الحصول عليها بعد التجفيف وجمعها من رقائق الألومنيوم إلى حاوية محكمة الإغلاق. تم تمييز الألياف النانوية باستخدام مطياف الأشعة تحت الحمراء بتحليل الانعكاس الكلي المخفف (FTIR) للكشف عن وجود بوليمر الزين في المصفوفة. ثم تم تحليل شكل سطح الألياف النانوية باستخدام تقنية المجهر الإلكتروني الماسح (SEM) لتوضيح التغيرات المورفولوجية في الألياف النانوية الناتجة.

النتائج:

أشارت النتائج إلى أن بعض المعلمات والظروف المحددة يمكن أن تؤدي إلى تشكيل ألياف نانوية بشكل مثالي، وأن تطبيق ظروف ومعلمات مختلفة يمكن أن يؤدي إلى تضاريس مورفولوجية غير طبيعية ورش كهربائي بدلاً من ألياف نانوية مغزولة كهربائيًا.

الاستنتاجات:

قدمت صور المجهر الإلكتروني الماسح (SEM) دليل بصريًا على التغير في الشكل المورفولوجي الناتج في كل تجربة مختلفة مع ظروف ومعلمات مختلفة

هدف الدراسة:

هدفت هذه الدراسة إلى تحديد تأثير معلمات الغزل الكهربائي والمعلمات البيئية المختلفة على الألياف النانوية لبوليمر الزين الناتجة.

1. Introduction

The electrospinning technique is one of the methods that have been used to prepare different types of nanofibers using high voltage to create surface tension at the droplet of the polymeric liquid at the needle tip, leading to the formation of a Taylor cone. This leads to the release of the solution finely charged polymeric jet forming nanofibers at rotating or adjusted collection surfaces (Abdulhussain et al. 2023). The electrospinning process is affected by several parameters that can change the morphology of the resulting nanofiber. In some cases, it leads to the formation of electro-spraying (Deitzel et al. 2001). Zein is a biopolymer obtained from protein in maize starch (Deitzel et al. 2001; Tortorella et al. 2021; Abdulhussain et al. 2023). It can form nanofibers used in topical and systemic sustained release of accompanied drugs loaded within it (Tortorella et al. 2021). Preparing the nanofibers of this polymer in different types of dosage forms using electrospinning technology made a critical focus on what the specified parameters used to get the perfect nanofibers and what the impact of these parameters on the resulting nanofibers leading to the development of fiber-based drug delivery systems (Tortorella et al. 2021).
The study employed the electrospinning technique in different parameter settings to create nanofiber mats made of zein to explain the effect of parameters on the morphological results of nanofibers (Lasprilla-Botero et al. 2018).

2. Materials and Methods

2.1.Materials: The Zein polymer was acquired from Sigma Aldrich in the United States.

2.2.Methods

2.2.1. Preparation of Nanofiber Solution

A solution was created by dissolving at 1g per 5 ml. The solution comprised 50 ml of 100% ethanol and distilled water (DW), then gentle stirring for one hour to ensure complete dissolution. Subsequently, 3 ml of the polymeric was loaded into a 3 ml syringe.

2.2.2. Preparations of Nanofibers by Electrospinning

At the beginning of the electrospinning process, the electrospinning apparatus, consisting of a syringe pump (New Era pump system, USA) and locally developed and assembled components, was configured to adjust all parameters and introduce one different parameter each run during the entire run. Then, the 3 ml syringe was placed in the syringe pump using different gages, and the applied voltage was adjusted, as well as the distance between the needle tip and collector, the flow rate of polymeric liquid, and the environmental humidity, the temperature recorded these adjustment ware made in each run as described in the Fig.1 (Dai et al. 2014; Abu Owida et al. 2022; Nguyen et al. 2023).

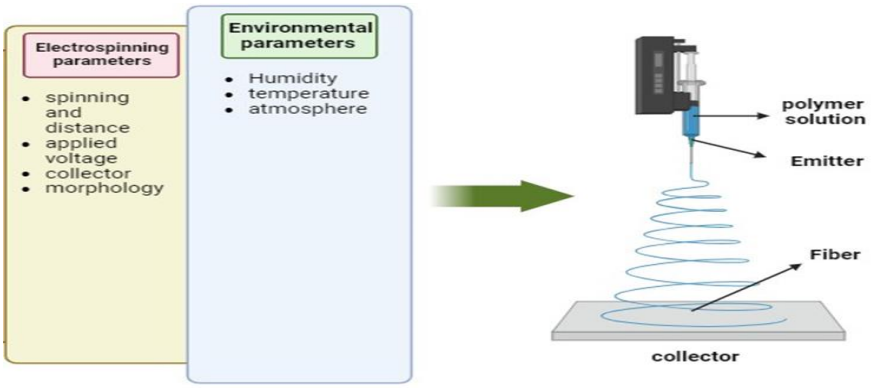

Figure 1: Shows the various parameters influencing the resulting nanofibers, including Electrospinning Parameters and Environmental Parameters.

2.2.3. Fourier Transforms Infrared Spectroscopy (FTIR)

A nanofiber sample was applied onto a petri dish and subsequently examined utilizing FTIR analysis with the assistance of an FTIR spectrophotometer (Bruker-Optic162, Germany). The 10 mg zein nanofibers were placed onto the lens. It was then mixed with 10 mg of potassium bromide (KBr) and fitted into the lens. The chart was created with a resolution of 2 cm-1. FTIR spectrophotometer measured values within the 3500 to 400 cm-1 range (Kamnev et al. 2021). To ensure the precise delivery of the provided formula without any possible interactions (Dai et al. 2014; Kamnev et al. 2021; Nguyen et al. 2023).

2.2.4. FESEM Analysis of Resulted Nanofibers

The morphologic surface topography of the nanofibers was obtained using field emission scanning electron microscopy (FESEM) instrument (FE Axia chem SEM, thermos fisher Holand). The settings of the scanning electron microscope (SEM) were adjusted at an applied voltage of 10 kilovolts (kV) and a surface distance of 5.71 millimeters (mm). A small piece of nanofibers covered with gold (Au) using a sputter-coating technique. Fiber diameter was measured using the Picture J software, applying it to 24 fiber sections derived from a scanning electron microscopy (FESEM) image (Van Roon et al. 2005; Gnanamoorthy et al. 2014).

2.2.5. The Adjustment of Parameters

An 18-run with an electrospinning device was conducted by selecting the most appropriate formula through its FESEM morphological results run 7. The parameters are fixed in each run depending on the best results, changing only one parameter, as shown in Table 1.

Table 1: The Different Ranges of Electrospinning and Environmental Parameters Were Applied in Each Run, Noticing That the Best Run Was No 7, Fixed in All Runs, Changing Only One Parameter at a Time

Run	Electrospinning parameters				Environmental Parameters	
	Flow rate (ml/h)	Syringe gage	Distance between needle tip and collector (Cm)	Applied voltage (Kv)	Temperature (C°)	Humidity (%)
1	0.5	18	17	15.7	30	26.6
2	0.8	18	17	15.7	30	26.6
3	1	18	17	15.7	30	26.6
4	0.6	15	17	15.7	30	26.6
5	0.6	20	17	15.7	30	26.6
6	0.6	22	17	15.7	30	26.6
7	0.6	18	17	15.7	30	26.6
8	0.6	18	17	15.7	13.8	26.6
9	0.6	18	17	15.7	45	26.6
10	0.6	18	17	24	30	26.6
11	0.6	18	17	19	30	26.6
12	0.6	18	17	15	30	26.6
13	0.6	18	17	15.7	30	71
14	0.6	18	17	15.7	30	47
15	0.6	18	17	15.7	30	20.1
16	0.6	18	15	15.7	30	26.6
17	0.6	18	10	15.7	30	26.6
18	0.6	18	13	15.7	30	26.6

3. Results and Discussion:

3.1.Fourier Transform Infrared Analysis

An analysis of the FTIR spectrum was conducted to identify the specific peaks occurring at different bandwidth intervals in nanofibers-impregnated Zein. To ensure the presence of Zein in each resulting nanofiber without any change. Zein has four distinct bands that accurately reflect its protein composition. 2800 to 3500 cm−1 spectral range corresponds to N-H and O-H bonds vibrational stretching represents the protein amino acids. Amide band spectral characteristic at a wavelength of 1658 cm−1, ascribed to the elongation of the carbonyl (C=O) bonds inside the amide groups of the peptide moieties, namely in the amide I region. At the same time, it represents the amide II at a wavenumber of 1541 cm−1. This specific band is linked to the angular deformation vibrations of the N-H bond. The axial deformation vibrations of the C-N bond appeal at 1238 cm−1 (Gough et al. 2020; Sadat and Joye 2020), as shown in Fig.2.

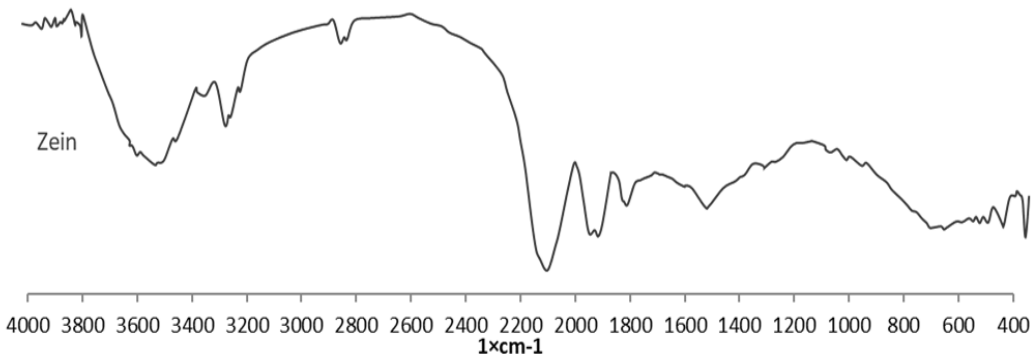

Figure 2: FT-IR spectrum of zein nanofibers, showing distinctive wavelengths corresponding to amide and amine groups within the amino acids that make up the protein moiety of zein

3.2.FESEM Analysis of Different Runs

After the fixation of the run (7) parameters, which is the best-selected formula that has uniform, beadles, transparent fibers at the sizes of around 310nm to 340nm, by changing one parameter at a time in each run, the results show different patterns of nanofibers and electro spraying (no nanofiber result). Results show distinct patterns of morphological aspects in each run when a parameter changes. By changing the flow rate of the syringe pump at different levels (0.5, 0.8, and 1 ml/h), as shown in runs (1, 2, and 3), the resulting nanofibers tend to be more uniform and well-shaped when the flow rate is reduced as shown in Fig.3. That's due to the increased injected liquid from the syringe at the unit time, leading to the deformity of the trajectory jet and Taylor cone. This result shows a correlation to Zergham et al (Yarin, Koombhongse and Reneker, 2001; Jalili, Morshed and Ravandi, 2006).

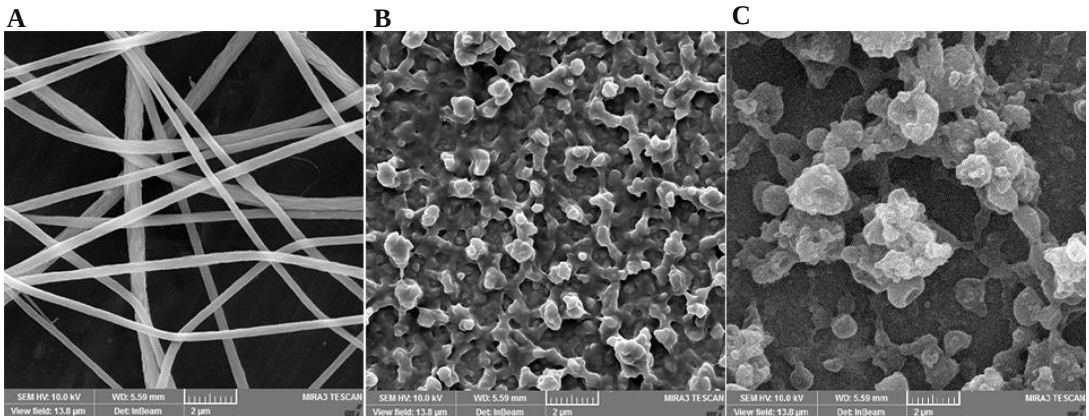

Figure 3: FESEM images depict the morphological changes in nanofibers resulting from adjustments to the syringe pump flow rate: **(A)** 0.5 mL/h, **(B)** 0.8 mL/h, and **(C)** 1 mL/h.

While the adjustment of the syringe gage of runs (4, 5, and 6), the resulting nanofibers show a lack of correlation between the syringe gage and nanofibers morphology. These three runs' nanofibers show excellent characteristics, as shown in Fig.4. These results confirm the results showed by Macossay *et al.* (Macossay et al. 2007)

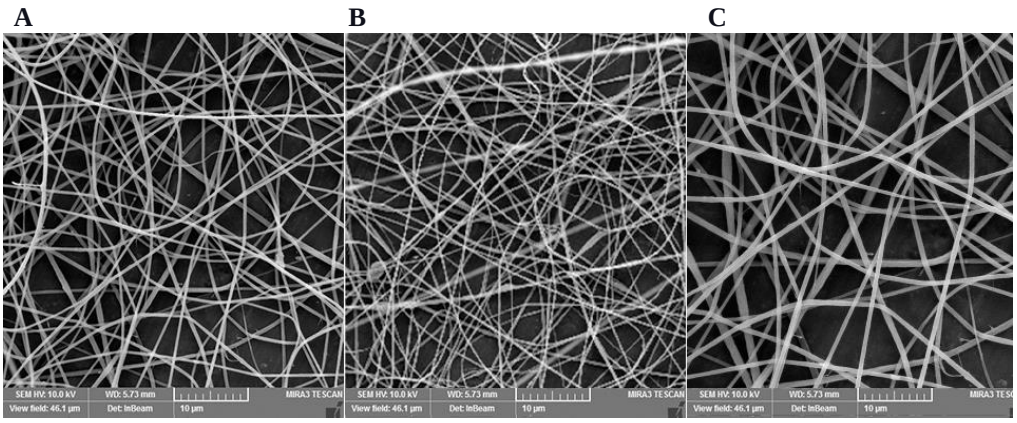

Figure 4: FESEM images show no morphological changes with adjustments in syringe gauge: **(A)** Gauge 15, **(B)** Gauge 20, and **(C)** Gauge 22.

Decreasing the distance between the needle tip and the collector for both the plane and roller collector in runs (16,17, and 18) tends to affect the morphology of the resulting nanofiber. Reducing the distance will lead to bead formation and irregular distribution of the fibers, as shown in Fig.5, which refers to the short time that the fibers take to travel to the collector and, hence, low time for drying before reaching the collector; these results are confirmed by Xue and his colleague (Jalili et al. 2006; Ferrández-Rives et al. 2017; Yousefi et al. 2018).

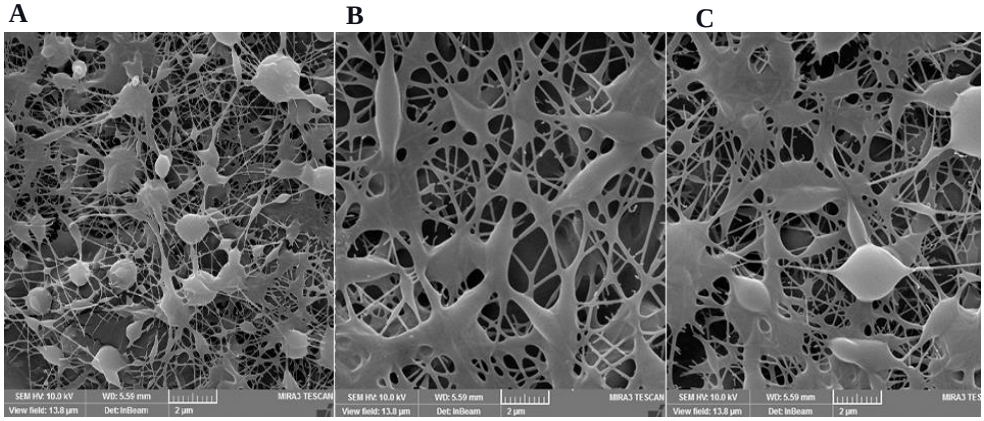

Figure 5: FESEM images display significant morphological changes due to adjustments in the distance between the needle tip and collector: **(A)** 15 cm, **(B)** 10 cm, and **(C)** 13 cm.

An elevation in the applied voltage can result in the formation of beads. With continuous release, the fibers disappear, forming clusters due to electrospraying in run (10, 11, and 12); the differences in the morphology can be seen in Fig.6. These results also appear with previously published data (Ferrández-Rives et al. 2017; Xue et al. 2019a; Xue et al. 2019b).

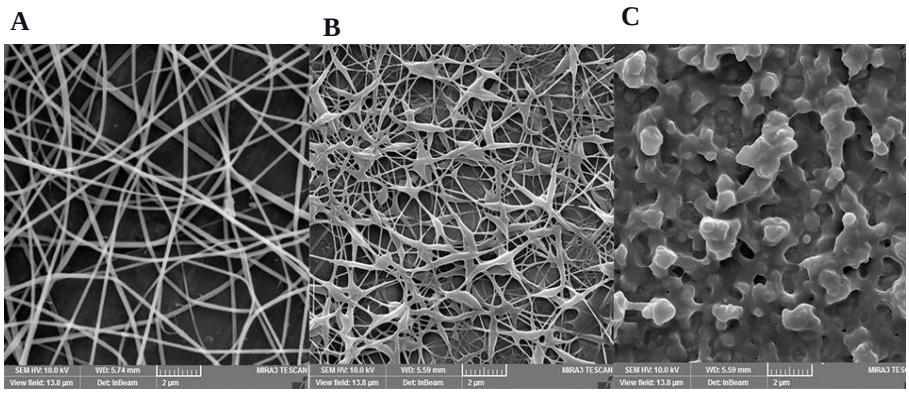

Figure 6: FESEM images reveal significant morphological changes due to adjustments in the applied voltage: **(A)** 15 kV, **(B)** 19 kV, and **(C)** 24 kV.

Decreasing the temperature results in beads due to the decrease in the drying time of the nanofibers plus the increase in viscosity, which can be seen in the run (8). In contrast, the slight elevation in temperature results in an excellent fine nanofiber due to the decrease in viscosity and surface tension, as shown in run (10); very elevated lab temperature led to the premature termination of the fluid jet electrical stretching, as can be seen in run (9) all these results shown in Fig.7. These results are similar to the findings that published by Yang et al. (De Vrieze et al. 2009; Yang et al. 2017; Refate et al. 2023)

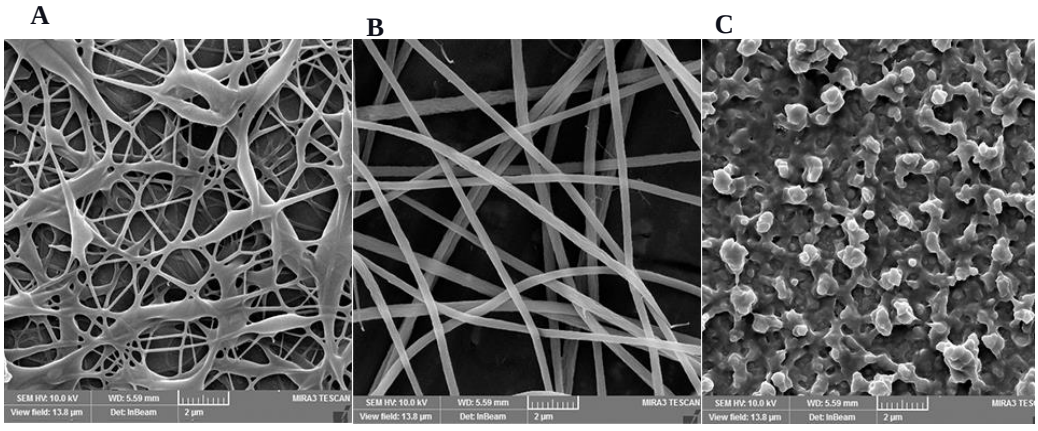

Figure 7: FESEM images show significant morphological changes due to variations in working temperatures and their impact on the resulting nanofibers: **(A)** 13.8°C, **(B)** 30°C, and **(C)** 45°C.

Increased humidity can influence the diameter of electrospun nanofibers. Decreased relative humidity leads to quicker solvent loss, resulting in thicker nanofibers in the run (15 and 14). Conversely, increased humidity hinders the process

of solvent evaporation, leading to the production of thinner nanofibers in the run (13). All these results are shown in Fig.8. These results are highly relative to the findings of Raska et al. (Raksa, Numpaisal and Ruksakulpiwat, 2021; Ura et al., 2021).

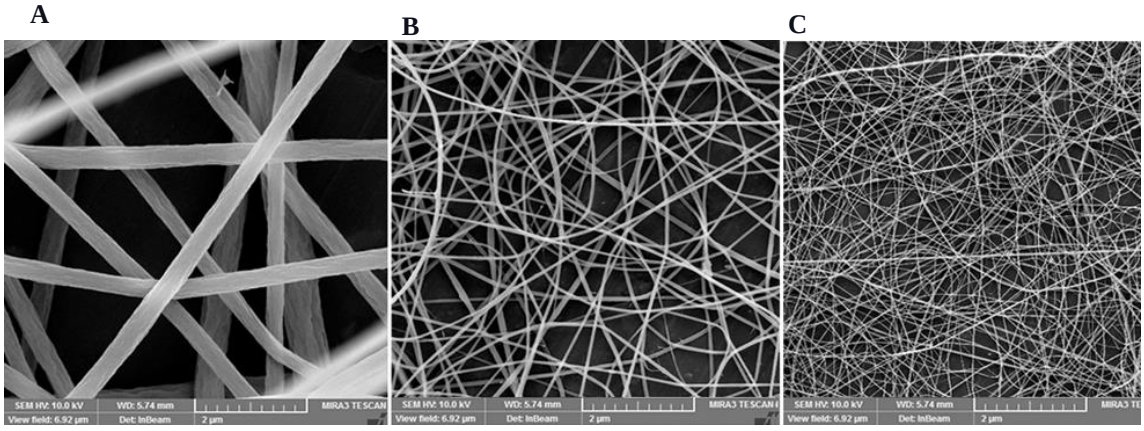

Figure 8: FESEM images reveal significant morphological changes due to variations in working humidity and their impact on the resulting nanofibers: **(A)** 20.1%, **(B)** 47%, and **(C)** 71%.

4. Conclusion

From the results of FESEM analysis, it's clear that electrospinning and environmental parameters have a very severe impact on the morphology of the resulting nanofibers, ranging from a deformity and bead formation to modification on the diameter and size; each modification in each of these factors can result in different results and hence different product, to prepare a specific zein nanofiber for whatever drug loading formula the parameters most adjusted to prepare the desired characteristics.

References

Abdulhussain, R., Adebisi, A., Conway, B.R. and Asare-Addo, K. 2023. Electrospun nanofibers: Exploring process parameters, polymer selection, and recent applications in pharmaceuticals and drug delivery. *Journal of Drug Delivery Science and Technology* 90. doi: 10.1016/j.jddst.2023.105156.

Abu Owida, H., Al-haj Moh'd, B. and Al Takrouri, M. 2022. Designing an Integrated Low-cost Electrospinning Device for Nanofibrous Scaffold Fabrication. *HardwareX* 11. doi: 10.1016/j.ohx.2021.e00250.

Dai, X., Kathiria, K. and Huang, Y.C. 2014. Electrospun fiber scaffolds of poly (glycerol-dodecanedioate) and its gelatin blended polymers for soft tissue engineering. *Biofabrication* 6(3). doi: 10.1088/1758-5082/6/3/035005.

Deitzel, J.M., Kleinmeyer, J., Harris, D. and Beck Tan, N.C. 2001. The effect of processing variables on the morphology of electrospun nanofibers and textiles. *Polymer* 42(1). doi: 10.1016/S0032-3861(00)00250-0.

Ferrández-Rives, M., Beltrán-Osuna, Á.A., Gómez-Tejedor, J.A. and Ribelles, J.L.G. 2017. Electrospun PVA/bentonite nanocomposites mats for drug delivery. *Materials* 10(12). doi: 10.3390/ma10121448.

Gnanamoorthy, P., Karthikeyan, V. and Prabu, V.A. 2014. Field emission scanning electron microscopy (FESEM) characterisation of the porous silica nanoparticulate structure of marine diatoms. *Journal of Porous Materials* 21(2). doi: 10.1007/s10934-013-9767-2.

Gough, C.R., Bessette, K., Xue, Y., Mou, X. and Hu, X. 2020. Air-jet spun corn zein nanofibers and thin films with topical drug for medical applications. *International Journal of Molecular Sciences* 21(16). doi: 10.3390/ijms21165780.

Jalili, R., Morshed, M. and Ravandi, S.A.H. 2006. Fundamental parameters affecting electrospinning of PAN nanofibers as uniaxially aligned fibers. *Journal of Applied Polymer Science* 101(6). doi: 10.1002/app.24290.

Kamnev, A.A., Dyatlova, Y.A., Kenzhegulov, O.A., Vladimirova, A.A., Mamchenkova, P. V. and Tugarova, A. V. 2021. Fourier transform infrared (FTIR) spectroscopic analyses of microbiological samples and biogenic selenium nanoparticles of microbial origin: Sample preparation effects. *Molecules* 26(4). doi: 10.3390/molecules26041146.

Lasprilla-Botero, J., Álvarez-Láinez, M. and Lagaron, J.M. 2018. The influence of electrospinning parameters and solvent selection on the morphology and diameter of polyimide nanofibers. *Materials Today Communications* 14. doi: 10.1016/j.mtcomm.2017.12.003.

Macossay, J., Marruffo, A., Rincon, R., Eubanks, T. and Kuang, A. 2007. Effect of needle diameter on nanofiber diameter and thermal properties of electrospun poly(methyl methacrylate). *Polymers for Advanced Technologies* 18(3), pp. 180–183. doi: 10.1002/PAT.844.

Nguyen, T.D., Roh, S., Nguyen, M.T.N. and Lee, J.S. 2023. Structural Control of Nanofibers According to Electrospinning Process Conditions and Their Applications. *Micromachines* 14(11). doi: 10.3390/mi14112022.

Raksa, A., Numpaisal, P.O. and Ruksakulpiwat, Y. 2021. The effect of humidity during electrospinning on morphology and mechanical properties of SF/PVA nanofibers. In: *Materials Today: Proceedings*. doi: 10.1016/j.matpr.2021.03.459.

Refate, A. et al. 2023. Influence of electrospinning parameters on biopolymers nanofibers, with emphasis on cellulose & chitosan. *Heliyon* 9(6). doi: 10.1016/j.heliyon.2023.e17051.

Van Roon, J.L., Van Aelst, A.C., Schroën, C.G.P.H., Tramper, J. and Beeftink, H.H. 2005. Field-emission scanning electron microscopy analysis of morphology and enzyme distribution within an industrial biocatalytic particle. *Scanning* 27(4). doi: 10.1002/sca.4950270405.

Sadat, A. and Joye, I.J. 2020. Peak fitting applied to fourier transform infrared and raman spectroscopic analysis of proteins. *Applied Sciences (Switzerland)* 10(17). doi: 10.3390/app10175918.

Tortorella, S., Maturi, M., Vetri Buratti, V., Vozzolo, G., Locatelli, E., Sambri, L. and Comes Franchini, M. 2021. Zein as a versatile biopolymer: different shapes for different biomedical applications. *RSC Advances* 11(62). doi: 10.1039/d1ra07424e.

Ura, D.P. et al. 2021. Surface Potential Driven Water Harvesting from Fog. *ACS Nano* 15(5). doi: 10.1021/acsnano.1c01437.

De Vrieze, S., Van Camp, T., Nelvig, A., Hagström, B., Westbroek, P. and De Clerck, K. 2009. The effect of temperature and humidity on electrospinning. *Journal of Materials Science* 44(5). doi: 10.1007/s10853-008-3010-6.

Xue, J., Wu, T., Dai, Y. and Xia, Y. 2019a. Electrospinning and electrospun nanofibers: Methods, materials, and applications. *Chemical Reviews* 119(8). doi: 10.1021/acs.chemrev.8b00593.

Xue, J., Wu, T., Dai, Y. and Xia, Y. 2019b. Electrospinning and electrospun nanofibers: Methods, materials, and applications. *Chemical Reviews* 119(8). doi: 10.1021/acs.chemrev.8b00593.

Yang, G.Z., Li, H.P., Yang, J.H., Wan, J. and Yu, D.G. 2017. Influence of Working Temperature on The Formation of Electrospun Polymer Nanofibers. *Nanoscale Research Letters* 12(1). doi: 10.1186/s11671-016-1824-8.

Yarin, A.L., Koombhongse, S. and Reneker, D.H. 2001. Taylor cone and jetting from liquid droplets in electrospinning of nanofibers. *Journal of Applied Physics* 90(9). doi: 10.1063/1.1408260.

Yousefi, S.H., Venkateshan, D.G., Tang, C., Tafreshi, H.V. and Pourdeyhimi, B. 2018. Effects of electrospinning conditions on microstructural properties of polystyrene fibrous materials. *Journal of Applied Physics* 124(23). doi: 10.1063/1.5049128.